Interaction between Emulsion Droplets in the Presence of Polymer−Surfactant Complexes

ARTICLE *in* LANGMUIR · MAY 2002

Impact Factor: 4.46 · DOI: 10.1021/la0256477

6 AUTHORS, INCLUDING:

John Philip
Indira Gandhi Centre for Atomic Research
179 PUBLICATIONS **3,142** CITATIONS

Interaction between Emulsion Droplets in the Presence of Polymer−Surfactant Complexes

John Philip,*,† G. Gnana Prakash,† T. Jaykumar,† P. Kalyanasundaram,† O. Mondain-Monval,‡ and Baldev Raj†

DPEND, Indira Gandhi Centre for Atomic Research, Kalpakkam 603 102, India, and Centre Recherche Paul Pascal, Avenue Albert Schewitzer, 33600 Pessac, France

Received February 21, 2002. In Final Form: March 31, 2002

The interaction between liquid−liquid dispersion covered with polymer−surfactant complexes has been in investigated. The polymer used for our investigations is poly(vinyl alcohol) and the surfactants were sodium dodecyl sulfate, cetyltrimethylammonium bromide and tetradecyltrimethylammonium bromide, and nonyl phenol ethoxylate (NP10). It has been found that the magnitude and the onset of repulsive forces increase dramatically during the association process. The onset of association depends on the nature of surfactant and interfacial properties of the emulsion droplet. The force profiles follow an exponential scaling with a characteristic decay length equal to the R_g of the polymer, irrespective of the surfactant concentration. No associative behavior has been observed in the presence of nonionic surfactant (NP10). The experimental observations suggest that in the presence of charged surfactant molecules or micelles, the neutral polymer chains at the interface are converted into partial polyelectrolytes, where the charges on the chain repel each other and the electrostatic repulsion collectively leads to chain stretching, which would provide better stability to the colloidal particles.

Introduction

The ability of polymer−surfactant complexes to alter the rheological properties of aqueous solutions in many formulations in the area of medicine, food, detergent, enhanced oil recovery, cosmetics, etc. has been a topic of intense research for the last few decades.[1−33] Understanding the associative behavior of such polymer−surfactant complexes is not only of fundamental interest but also important in many industrial applications. There are numerous studies to obtain insights into the polymer−surfactant or polyelectrolyte−surfactant complexes, using various experimental techniques.[13−21]

Force measurement techniques have been widely used to gain insights into the colloidal stability. The net force acting between the colloidal particles determines the stability of the colloidal system. The most important forces that determine the stability of the colloidal dispersions are van der Waals attractive forces, electrostatic forces, and steric forces due to the adsorbed polymers. Although, stabilization of the colloidal dispersions with macromolecules has been explored in various technological applications for many years, the interactions between polymer-bearing surfaces have been studied directly only after the introduction of the surface force measurement apparatus.[28] Steric stabilization of the colloidal dispersions

* To whom correspondence may be addressed. E-mail: philip@igcar.ernet.in.

† DPEND, Indira Gandhi Centre for Atomic Research.

‡ Centre Recherche Paul Pascal.

(1) *Interactions of surfactants with polymers and proteins;* Goddard, E. D., Anadapadmanabhan, K. P., Eds.; CRC Press: Boca Raton, FL, 1993.

(2) In *anionic surfactant Physical Chemistry of surfactants Action*; Lucassen-Reynders, E. H., Robb, I. D., Eds.; Marcel Deckker: New York, 1981.

(3) Thalberg, K.; Lindman, B. In *Surfactants in Solution*; Mittal, K. L., Shah, D. O., Eds.; Plenum: New York, 1991.

(4) Chang, Y.; Lochead, R. Y.; McCormick, C. L. *Macromolecules* **1994**, *27*, 2145.

(5) Goddard, E. D.; Phillips, T. S.; Hannan, R. B. *J. Soc. Cosmet. Chem.* **1975** *26*, 461.

(6) Goddard, E. D.; Leung, P. S. *Polym. Prepr.* (*Am. Chem. Soc., Div. Polym. Chem.*) **1982**, *23*, 47.

(7) Iliopoulos, I.; Wang, T. K.; Audebert, R. *Langmuir* **1991**, *7*, 617.

(8) Mangy, B.; Iliopoulos, I.; Audebert, I.; Piculell, R.; Lindman, L. B. *Prog. Colloid Polym. Sci.* **1992**, *89*, 118.

(9) de Gennes, P. G. *J. Phys. Chem.* **1990**, *94*, 8407.

(10) Nikas, Y. J.; Blankschtein, *Langmuir* **1994**, *10*, 3512.

(11) Antony, O.; Zana, R. *Langmuir* **1994**, *10*, 4048; **1996**, *12*, 3590; **1996**, *12*, 1967.

(12) Ruckenstein, E. *Langmuir* **1999**, *15*, 8086.

(13) Jones, M. N. *J. Collid Interface Sci.* **1967**, *23*, 36.

(14) Cabane, B. *J. Phys. Chem.* **1977**, *81*, 1639; *J. Phys.* **1982**, *43*, 1529; *Colloids Surf.* **1985**, *13*, 19.

(15) Xia, J.; Dublin, P. L.; Kim, Y. *J. Phys. Chem.* **1992**, *96*, 6805.

(16) Effing, J. J.; MacLennan, I. J.; Kwak, J. C. T. *J. Phys. Chem* **1994**, *98*, 2550.

(17) Cosgrove, T.; Mears, S.; Thompson, J. L.; Howell, I. *ACS Symp. Ser.* **1995**, *No. 615*, 196.

(18) Lee, L. T.; Cabane, B. *Macromolecules* **1997**, *30*, 6559; *Curr. Opinion. Colloid Sci.* **1999**, *4* 205. (See this reference for a comprehensive review on small-angle neutron scattering studies on polymer surfactant mixtures.)

(19) Purcell, I. P.; Lu, J. R.; Thomas, R. K.; Howe, A. M.; Penfold, J. *Langmuir* **1998**, *14*, 1637.

(20) Staples, E.; Tucker, I.; Penfold, J.; Warren, N.; Thomas, R. K. *J. Phys. Condens. Matter* **2000**, *12*, 6023.

(21) Millet, F.; Benatter, J. J.; Perrin, P. *Phys. Rev. E* **1999**, *60*, 2045.

(22) Dhara, D.; Shah, D. O. *J. Phys. Chem. B* **2001**, *5*, 61.

(23) Zhu, P. W.; Napper, D. H. *Phys. Rev. E* **2000**, *61*, 2859; **2000**, *61*, 6866.

(24) Wesley, R. D.; Cosgove, T.; Thompson, L. *Langmuir* **1999**, *15*, 8376.

(25) Folmer, B. M.; Kronberg, B, *Langmuir* **2000**, *16*, 7168.

(26) Robb, I. D.; Stevenson, P. *Langmuir* **2000**, *16*, 5987.

(27) Smith, G. L.; McCormick, C. L. *Langmuir* **2001**, *17*, 1719. (This group has published a series of articles on this topic under the title water-soluble polymer.)

(28) Israelachvili, J. N.; Tabor, D. *Proc. R. Soc. London, Ser. A.* **1972**, *19*, 331. Israelachvili, J. N.; Adams G. E. *J. Chem. Soc., Faraday Trans. 1* **1978**, *74*, 975.

(29) Klien, J.; Luckham, P. *Nature* **1984**, *308*, 836. Luckham, P F.; Klien, J. *J. Chem. Soc., Faraday Trans. 1* **1984**, *80*, 865.

(30) *Polymeric stabilization of collidal dispersions*; Napper, D. H., Ed.; Academic Press: New York, 1983.

(31) Philip, J.; Bonakdar, L.; Poulin, P.; Bibette, J.; Leal Calderon, F. *Phys. Rev. Lett.* **2000**, *84*, 2018. Philip, J.; Poirier, J. E.; Bibette, J.; Leal Calderon, F. *Langmuir* **2001**, *17*, 3545.

(32) *Intermolecular and Surface Forces*; Israelachvili, J. N., Ed.; Academic Press: San Diego, CA, 1985.

(33) *Polymers in colloidal systems*; Tadors, Th., Ed.; Elsevier: Amsterdam, 1983. *Solid-state dispersions*; Academic Press: New York, 1988.

10.1021/la0256477 CCC: $22.00
Published on Web 05/09/2002

has triggered a lot of interest in recent years due to its several advantages over its electrostatic counterpart and more importantly due to its numerous industrial applications.[29,30] It is well-known that electrostatically stabilized colloids often coagulate when the ionic strength of the medium is increased sufficiently, due to the reduction in the spatial extension of the electrical double layers.[31] One major advantage of using macromolecules as stabilizers is that the double layers are less sensitive to electrolyte concentration. The understanding of forces between surfactant- and polymer-covered interfaces has been investigated thoroughly using various force measurement techniques; as a result, this topic is rich and understood to a great extent.[32−34]

Compared to the understanding of forces in the presence of surfactants or polymers, the understanding of polymer−surfactant complexes is still in its infancy. In recent years, there have been some attempts to explore the forces in the presence of associative polymers and polyelectrolytes.[35−40] The effect of an anionic surfactant to the forces between surfaces precoated with a high charge density cationic polyelectrolyte was investigated by Claesson.[35] Similarly the associative behavior of ionic surfactants and polylectrolytes has been studied.[36] Atomic force microscopy is also employed to investigate the interaction forces between a mica surface and a colloidal glass sphere in the presence of a high molecular weight cationic polyelectrolyte and an anionic surfactant.[37] Most of the force measurements have been carried out by using the surface force apparatus (SFA). Numerous other approaches have also been invented for measuring surface forces directly and indirectly. Recently a new technique,[41−44] called magnetic field induced chaining technique (MCT) has been introduced to probe the forces between tiny colloidal particles. In the case of SFA, the force is measured between semimacroscopic surfaces (mica) whereas in MCT, the forces between individual colloidal droplets are measured. Using this technique, one can measure the colloidal forces in a wide variety of materials encountered in emulsions and dispersions.

Although there are numerous studies on the associative behavior of polymers in bulk solutions,[4−27] there are no reports on the nature of association, when the associative polymers adsorb irreversibly or reversibly at the interface of colloidal particles. Probably this is due to the lack of an experimental tool to investigate this aspect. Here, using the new force measurement approach,[41−44] we have been successful in investigating the role of associative polymers on colloidal stability. In this paper, we report some insights into the polymer−surfactant association process and its influence on long-term stability of emulsions.

Experimental Section

Materials. Direct emulsion of ferrofluid was used in the present studies. Ferrofluid oil consists of a collection of ferromagnetic domains Fe_2O_3, of about 10 nm size, dispersed in octane.[45] The inner surfactant used to stabilize the oxide particles against van der Waals attraction was oleic acid. Monodispersed emulsions with narrow size distributions were obtained using a fractionation technique. The size distribution of the final emulsion has been measured by using a Malvern Instruments Master sizer. Emulsion droplets with a diameter of about 200 nm have been used in our studies. An optical phase contrast microscope (M/s Leica DM IRM) equipped with a digital camera (JVC) and imaging software (Leica) has been used for micromanipulation of the emulsion droplets.

The polymer used in these experiments was a statistical copolymer of vinyl alcohol (CH_2CHOH, 88%) and vinyl acetate ($CH_2CHOCOCH_3$), 12%), which is randomly distributed along the polymer chain, of average molecular weights of 155 000 (here after referred to as 155K). Here the former is hydrophilic and the later is hydrophobic in nature. These polymers are water soluble at room temperature and the theta temperature of PVA-vac in water is around 97 °C. By variation of the content of acetate, the hydrophobicity of the polymer can be altered. Both these polymers were obtained from Aldrich, USA, and were used as such. The R_g of these polymers was obtained from the hydrodynamic radii measurements. The experiments were carried out at a concentration well below the overlap concentration (C^*). The polymer concentration was 0.5 wt % for both polymers. PVA is a neutral polymer and hence the electrostatic effect need not be considered in the interpretation.

Surfactants used in our experiments, sodium dodecyl sulfate ($C_{12}H_{25}-SO_4Na$), cetyltrimethylammonium bromide ($CH_3-(CH_2)_{15}N(CH_3)_3Br$ hereafter referred to as CTAB), tetradecyltrimethylammonium bromide ($CH_3(CH_2)_{13}N(CH_3)_3Br$ hereafter referred to as TTAB), and nonyl phenol ethoxylate ($C_9H_{19}C_6H_4-(OCH_2CH_2)_{10}-OH$, hereafter referred as NP10) were obtained from Sigma. The purity of these chemicals was 99.9%, and they were used without any further purification. Triply distilled water (resistance value of 18.2 MΩ cm^{-1}) filtered with a 0.22 μm Millipore filter was used in the preparation of surfactant and polymer solutions.

Force Measurement. Details of the experimental technique are described in earlier publications.[41−44] The monodispersed emulsion is taken in an optical cell and is placed inside a solenoid-type electromagnet. The sample is illuminated by a halogen lamp. The light beam from the halogen source is steered into the sample cell by means of optical fibers, and the exact focusing is done by means of suitable optical components. The backscattered light from the sample is collected by means of optical fibers and sent into a monochromator equipped with 1024 diode array. The signal from the diode array is processed by a computer. Here, the exact spacing between the droplets is directly measured from the determination of the spectral distribution of the scattered light at a constant angle.

The principal of the force measurement approach is as follows. As the ferrofluid droplets are super-paramagnetic in nature, an applied field induces a magnetic dipole in each drop, causing them to form chains. Without an external field, these droplets have no permanent magnetic moments because of the random orientation of the magnetic grains within the droplets, due to thermal motion. An external magnetic field orients these magnetic grains slightly toward the field direction, which results in a dipole moment in each droplet. The magnitude of the magnetic dipole moment increases with the strength of the applied field until saturation is reached. At low concentration, one droplet thick chains are well separated and oriented along the field direction. Due to the presence of the one-dimensional ordered structure, a Bragg peak can be observed, from which the interdroplet separation is estimated precisely. The condition for forming a linear chain is that the repulsive force between the droplets must exactly balance the attractive force between the droplets induced by the applied magnetic field. The spacing between droplets is directly measured from the determination

(34) Patel, S.; Tirrell, M. *Annu. Rev. Phys. Chem.* **1989**, *40*, 597.
(35) Claesson, P. M.; Dedinite, P.; Blomberg, E.; Sergeyev, V. G. *Ber. Bensen-Ges. Phys. Chem.* **1996**, *100*, 1008.
(36) Fielden, M. L.; Claesson, P. M.; Schillen, K. *Langmuir* **1998**, *14*, 5366.
(37) Shubin, V.; Petrov, J.; Lindman, B. *Colloid Polym. Sci.* **1994**, *272*, 1590.
(38) Kjellim, U. R. M.; Claesson, P. M.; Audebert, R. *J. Colloid. Interface Sci.* **1997**, *190*, 476.
(39) Shuvin, V. *Langmuir* **1994**, *10*, 1093.
(40) Bremmele, K. E.; Jameson, G. J.; Biggs, S. *Colloid Surf., A* **1999**, *155*, 1.
(41) Leal-Calderon, F.; Stora, T.; Mondain Monval, O.; Bibette, J. *Phys. Rev. Lett.* **1994**, *72*, 2959.
(42) Mondain-Monval O.; Espert, A.; Omerjee, P.; Bibette, J.; Leal Calderon, F.; Philip, J.; Joanny, J. F. *Phys. Rev. Lett.* **1998**, *80*, 1778; **1995**, *75*, 3364.
(43) Philip, J.; Mondain Monval, O.; Leal Calderon, F.; Bibette, J. *J. Phys. D*: *Appl. Phys.* **1997**, *30*, 2798; *Bull. Mater. Sci.* **1999**, *22*, 101.
(44) Espert, A.; Omerjee, P.; Bibette, J.; Leal Calderon, F.; Mondain Monval, O. *Macromolecules* **1998**, *31*, 7023.
(45) *Emulsions*; *Theory and Practice*; Becher, P., Ed.; Rheinhold: New York, 1965.

of the spectral distribution of the scattered light at a constant angle. For perfectly aligned particles with a separation "*d*", the first-order Bragg condition leads to $2d = \lambda_o/n$. Where n is the refractive index of the suspending medium ($n = 1.33$ for water) and λ_o is the wavelength of the light Bragg scattered at an angle of 180°. The peak position moves toward a smaller wavelength as the field is increased. Because the droplets are monodispersed and negligibly deformable owing to their large capillary pressure, the corresponding interfacial separation is $h = d - 2a$. The magnitude of the induced dipole is controlled by the strength of the applied field.

To form a stable chain of droplet, the repulsive force between the droplets must exactly balance the attractive force between the dipoles induced by the applied magnetic field.

The dominant force in a field-induced droplet chain is the dipole−dipole attraction. The van der Waals contribution also becomes significant at short distances. The attractive dipole force within an infinitely long chain is[46]

$$F_{\text{chain}} = -\sum_{n=1}^{\infty} n\,\frac{6m^2}{(nd)^4} = -\zeta(3)\,\frac{6m^2}{d^4} \qquad (1)$$

where $\zeta(3) = \sum_{n=1}^{\infty} 1/n^3 = 1.202$ is the Riemann ζ function.

Here, m is the induced magnetic moment of each drop, which can be determined self-consistently from the intrinsic susceptibility of the ferrofluid, spherical shape of the drop, and presence of neighboring drops

$$m = \mu_0 4\pi a^3 \chi_s H_T/3 \qquad (2)$$

Here,"μ_0" is the magnetic permeability of free space and "H_T" is the total magnetic field acting on each drop. "χ_s" is the susceptibility of a spherical drop. Taking into account the demagnetization effect due to polarization

$$\chi_s = \frac{\chi}{1 + \frac{1}{3}\chi} \qquad (3)$$

Here "χ" is the intrinsic susceptibility of the fluid. H_T is the sum of the external applied field (H_{ext}) and the field from the induced magnetic moments (H_1) in all the neighboring drops in the chains. Due to strong surface tension, the elongation of the nanometer-sized droplet can be very small. According to a calculation[46] for a ferrofluid droplet of radius (r_0) 100 nm, at a magnetic field strength of 250 Oe, the eccentricity value is about 1.3×10^{-3}. This corresponds to the major axis "a" $= (1 + 4 \times 10^{-4})r_0$ and the minor axis "b" $= (1-2 \times 10^{-4})r_0$. Therefore, the elongation of the droplet is negligible.

For a droplet within an infinitely long chain of particles with equal spacing d, the total dipole field from all other particles is

$$H_1 = 2\sum_{n=1}^{\infty} \frac{2m}{(nd)^3} = 4\zeta(3)\,\frac{m}{d^3} \qquad (4)$$

Therefore, for an infinite dipole H_T becomes

$$H_T = H_{ext} + H_1 \qquad (5)$$

By use of eqs 1−5, the repulsive force between the droplet interfaces has been calculated. The multipole term has been neglected in these calculations, since its contribution is less than $10^{-3}F_m$.[46]

To study the effect of polymer adsorption of the force profiles, the emulsion stabilized with SDS at very low concentrations (cmc/50) is washed with PVA solutions of 0.5 wt % about four to five times. Then the emulsion is then incubated for about 48 h or more. No significant variations in the force profiles were noticed under these conditions. For association experiments, the required quantity of surfactants is added to the incubated emulsion. All the force measurement experiments have been performed at a temperature of 23 °C.

(46) Zhang, H.; Widom, M. *Phys. Rev. E* **1995**, *51*, 2099.

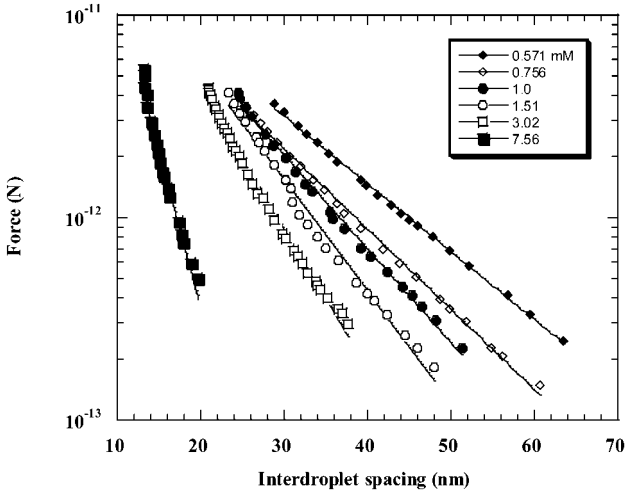

Figure 1. Shows force profiles in the presence of SDS at six different concentrations: 0.571, 0.756, 1.0, 1.51, 3.02, and 7.56 mM. The solid line represents the best fit obtained using eqs 6 and 8.

Results

Force Profiles in the Presence of Surfactants Alone. The initial emulsion is stabilized with SDS (anionic surfactant), and the droplet surface is negatively charged. Figure 1 shows the force profiles in the presence of SDS at different concentrations. The observed repulsive force profile was exponentially decaying. The repulsion comes from the charges at the interface of the droplets due to adsorption of charged surfactant molecules. The force profiles have been found to follow one of the electrostatic repulsive force equations depending[31,41] upon the "κa" values. When the droplet double layer is very thin, ($\kappa a <$ 5) the force profile follows the equation

$$F_r(d) = 4\pi\epsilon\psi_0^2 a^2\left[\frac{\kappa}{d} + \frac{1}{d^2}\right]\exp[-\kappa(d - 2a)] \qquad (6)$$

where ϵ is the dielectric permittivity of the suspending medium, ψ_0 is the electrical surface potential, and κ is the inverse Debye length, which essentially depends on the electrolyte concentration (C_s) and can be represented as

$$\kappa^{-1} = \left[\left(\frac{4\pi q^2}{\epsilon kT}\right)^2 C_s\right]^{-0.5} \qquad (7)$$

where "q" is the charge and kT is the thermal energy. For systems with a thin double layer ($\kappa a < 5$), the expression for the interaction force can be obtained by the Derjaguin approximation, where the surface potential is assumed to be constant and independent of the interparticle spacing h

$$F_r(d) = 2\pi\epsilon\psi_0^2 a\kappa\,\frac{\exp[-\kappa(d - 2a)]}{[1 + \exp(-\kappa(d - 2a))]} \qquad (8)$$

The intensity of the electrostatic forces is governed by the surface potential while the Debye length dictates the range of repulsion. The solid line in Figure 1 shows the best fit obtained. The unknown parameter in the theoretical equation is the surface potential, which was evaluated from the best fit. The experimental slopes for different surfactant concentrations were in good agreement with the theoretical slopes. The measured surface potential values were in good agreement with those values obtained independently from the electrophoresis mobility.

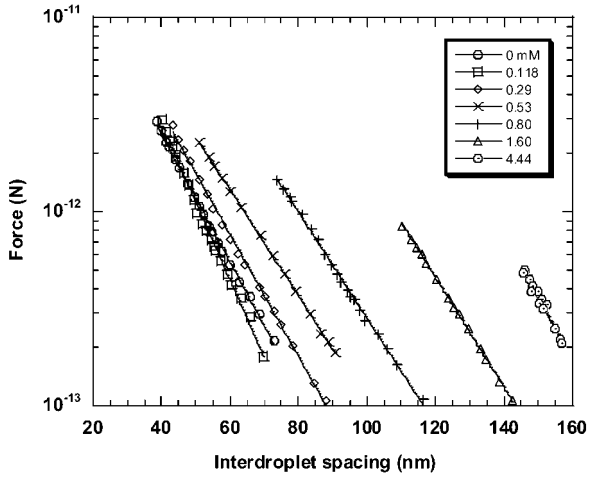

Figure 2. The variation of force profiles in the presence of PVA of 155K at a concentration of 0.5 wt % for sodium dodecyl sulfate concentrations of 0, 0.118, 0.29, 0.53, 0.80, 1.60, and 4.44 mM. The force profiles in the presence of PVA 155K of 0.5 wt % only correspond to 0 mM. The force profiles are repulsive and exponentially decaying with a characteristic decay length comparable to the R_g of the free polymer. The best fit (exponential) obtained using expression 9 is shown by the solid line.

Force Profiles in the Presence of Polymer Alone. The open circles in Figure 2 show the force profiles in the presence of PVA 155K. The force profiles are repulsive and exponentially decaying with a characteristic decay length close to the R_g of the free polymer. The exponential behaviors here are definitely not due to the electrostatic double layer forces due to parasitic charges since the slopes here are neither matching with the corresponding debye lengths nor sensitive to the addition of salt. For example, addition of 0.2 M NaCl into the emulsion does not change the slope of the force profiles. In fact, the Debye length for 0.1 M NaCl is 0.7 nm. The observed slope at this salt concentration was 14 nm for 155K. In fact, addition of salt slightly changes the solvent quality and the R_g of the polymer. The force profiles can be represented by a simple exponential function

$$F(h) = k \exp(-h/\lambda) \tag{9}$$

where "h" is the interdroplet spacing and "λ" is the decay length. These observations were consistent with the theoretical predictions obtained using both a mean field and a scaling approach.[42] The theory distinguishes the loops and tail sections of the adsorbed chains and involves three length scales, the adsorbed layer thickness λ, an adsorption length z^* that separates the regions where the monomer concentration is dominated by loops and by tails, and a microscopic length "b" inversely proportional to the adsorption strength. According to the mean field approach, in the strong adsorption limit ($\lambda/b \gg 1$), the expression for the adsorbed layer thickness, corresponding to the largest loops and tails in the layer, is given by

$$\lambda = \frac{R_g}{\left[\ln\left(\frac{1}{(\Phi_0 \nu b^2)}\right)\right]^{1/2}} \tag{10}$$

where ν is the Flory excluded volume parameter and Φ_0 is the bulk polymer volume fraction. According to the above expression, the adsorbed layer thickness is proportional to the R_g and weakly dependent on the adsorption strength and polymer concentration. At distances larger than λ, the concentration is dominated by the tails, and the force is always repulsive and decays exponentially with the distance. By using the Derjaguin approximation, in the scaling theory, we obtain the expression for force between two spherical droplets of radius R

$$F(h) = \frac{k_b T \pi R}{\lambda^2} \exp(-h/\lambda) \tag{11}$$

where k_b is the Boltzmann constant and T is the temperature. The above expression is valid only when the adsorbed polymer amount is close to the salutation value. The magnitude of the prefactor obtained from our experimental values very fairly matches (6×10^{-12} to 10^{-11} N) with the theoretically calculated values.

Force Profiles in the Presence of Surfactant−Polymer Complexes. Figure 2 shows the variation of force profiles in the presence of PVA of 155K at a concentration of 0.5 wt % for various sodium dodecyl sulfate concentrations. The critical micellar concentration (cmc) of SDS is 8×10^{-3} M. The surfactant concentrations were varied from about 0.118 to 4.44 mM. The force profile without any SDS (open circles in Figure 2) can be considered as the reference curve. The characteristic decay length without surfactant is 14 nm, which is close to the hydrodynamic R_g of the PVA measured using viscometry. In the presence of very small amounts of surfactant (0.118 mM), the force profile moved from the equilibrium position, without much variation in the decay length. Here the decay length increases slightly by about a few nanometers. However, the first interaction distance (which we defined as the distance at which the force value is 2×10^{-13} N, which is close to our detection limit of 10^{-13} N) increases by several nanometers. We should emphasize that the emulsion, normally became unstable at this concentration, without the presence of polymer. However, in the presence of polymer, the system remains stable for a long time and the force profiles remain the same even after several months. As the concentration of SDS increases further, both the magnitude and the first interaction distance increase drastically. The increase in the magnitude of force continues up to a value of 4.44 mM, which is close to cmc/2 for SDS. Due to some experimental limitation (poor efficiency of the holographic gratings and the photodiode array above the wavelength range of 1000 nm), we could not measure the force profiles above this SDS concentration. However, when we worked with polymers of lower molecular weights, we have seen a sort of saturation at around the cmc values.[47]

Figures 3 and 4 show the force profile in the presence of PVA with two cationic surfactants, cetyltrimethylammonium bromide (CTAB) and tetradecyltrimethylammonium bromide (TTAB), respectively. The critical micellar concentrations of CTAB and TTAB are 9×10^{-4} and 3.5×10^{-3} M, respectively. In the above two cases, the reference curves without any surfactant are shown in the figures (corresponding to 0 mM). The added surfactant concentrations are indicated in the inset box. In the case of CTAB, the onset of repulsion started to change at a surfactant concentration of 1.35 mM, which is roughly 1.5 times the cmc value. At concentrations below 1.5 cmc of CTAB, the force profiles remain the same, with respect to the reference curve. At surfactant concentration above 1.35 mM, the onset of repulsion and the magnitude of force profiles start to increase dramatically. The onset of repulsion has changed from about 60 to 155 nm when the surfactant concentration has been changed from 1.35 to

(47) Philip, J.; Jaykumar, T.; Kalynasundaram, P.; Raj, B.; Mondain-Monval, O. To be published. Philip, J. Patent pending.

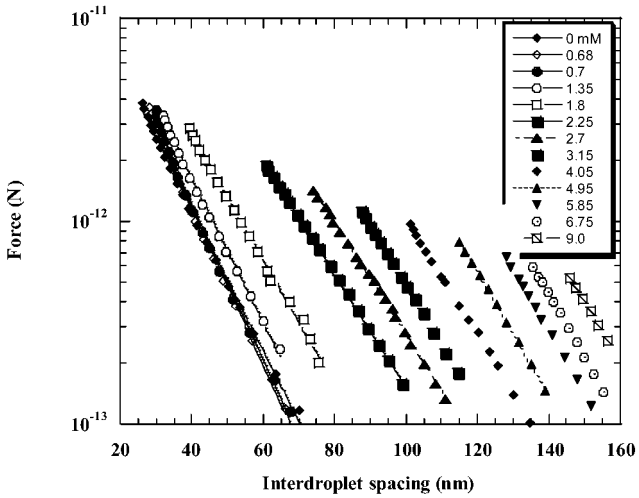

Figure 3. The force profile in the presence of PVA of 155K at a concentration of 0.5 wt % with a cationic surfactant (CTAB) of concentrations 0, 0.68, 0.7, 1.35, 1.8, 2.25, 2.7, 3.15, 4.05, 4.955, 5.85, 6.75, and 9 mM. The best fit (exponential) obtained by using expression 9 is shown by the solid line.

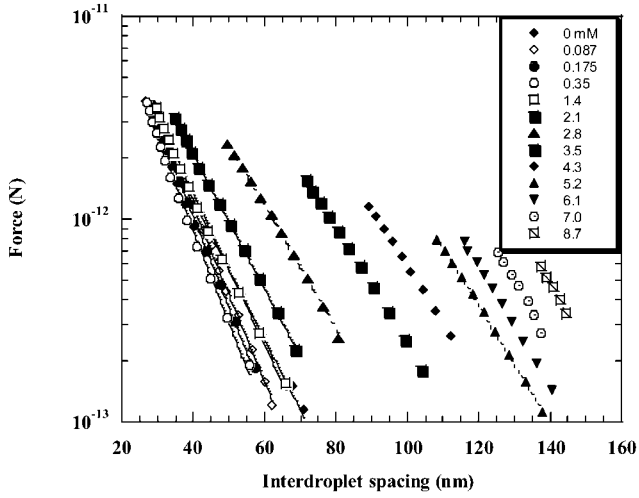

Figure 4. The force profile in the presence of PVA of 155K at a concentration of 0.5 wt % with a cationic surfactant (TTAB) at different concentrations of 0, 0.087, 0.175, 0.35, 1.4, 2.1, 2.8, 3.5, 4.3, 5.2, 6.1, 7.0, and 8.7 mM. The best fit (exponential) obtained using expression 9 is shown by the solid line.

9.0 mM (corresponding to 10cmc). This interdroplet spacing falls in the measurement limits of our force apparatus.

In the case of TTAB, variations in the force profiles begin at a surfactant concentration of 1.4 mM, which corresponds to cmc/2.5. The onset of repulsion and the magnitude of force monotonically increase above this surfactant concentration up to the detection limit. In this case, also the onset of repulsion has been increased from 60 nm to about 158 nm. At very low surfactant concentrations, the range of repulsion has slightly decreased but later followed the same trend as in the CTAB case.

In all three cases, where the surfactant molecules are ionic in nature, the force profile variation follows the same trend, expect for the concentration of surfactant at which the range of repulsion starts to vary. In the case of SDS, it happens at very low surfactant concentrations (cmc/68) where individual surfactant molecules are present in the system. Whereas in the cases of CTAB and TTAB, the onset of repulsion begins to change at surfactant concentrations close to the cmc value.

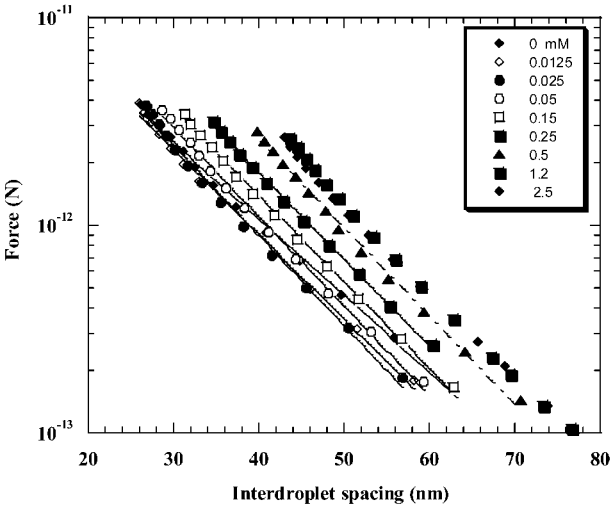

Figure 5. The force profiles in the presence of PVA of 155K at a concentration of 0.5 wt % with a nonionic surfactant, NP10. The surfactant concentrations are 0, 0.0125, 0.025, 0.05, 0.15, 0.25, 0.5, 1.2, and 2.5 mM The best fit (exponential) obtained using expression 9 is shown by the solid line.

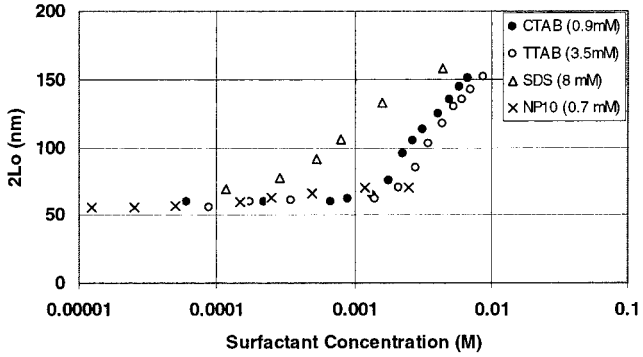

Figure 6. The variation in the onset of repulsion values ($2L_0$) as a function of surfactant concentrations for CTAB, TTAB, SDS, and NP10. The emulsion droplets are adsorbed with PVA of molecular weight 155K at a concentration 0.5%. The cmc values of the surfactants are cited in brackets.

Figure 5 shows the force profiles in the presence of the nonionic surfactant nonyl phenol ethoxylate (NP10). The critical micellar concentration is 7×10^{-4} M. Here, the force profiles do not show significant variations with surfactant concentration, which is varied from 0.125 to 2.5 mM (about 4cmc). Though the range of force has been increased slightly (about 10 nm), the variation was not significant with respect to the ionic surfactants. Figure 6 shows the variation in the onset of repulsion values ($2L_0$) for different surfactants used. It is clear that the variation is insignificant in the case of NP10, compared to the ionic surfactant. For ionic surfactants, it increases monotonically, above a particular surfactant concentration. The cmc values of the surfactants are mentioned in the inset. Figure 7 shows the variation in the decay length. In the case of cationic and anionic surfactants, the decay length increases first, reaches a maximum value, and then decreases. The total variation is about 5−6 nm in these cases, with respect to the unperturbed R_g values. In the case of nonionic surfactant, the decay length remains almost the same as the unperturbed R_g values. We have measured the R_g of the polymer with and without surfactant, using viscometry, and the R_g values obtained in these cases also followed the same trend.

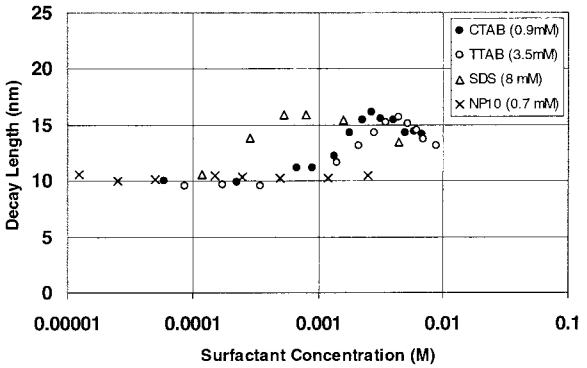

Figure 7. The variation in the decay length as a function of surfactant concentrations for CTAB, TTAB, SDS, and NP10. These values are obtained from the an exponential fit from Figures 2−5. The cmc values of the surfactants are cited in brackets.

Discussion

At the concentrations of polymer used in our experiments, the oil−water interface is fully covered with adsorbed polymer (i.e., the plateau region in the adsorption curve). This has been confirmed earlier from force measurement studies and from surface tension experiments.[44] Typical values of the adsorbed amount of polymers above the plateau concentration are about 1.5−2.2 mg/m^2. Normally, the polymer adsorbed at the oil−water interface adopt some arbitrary conformation with loops, trains, and tails (Figure 8a). Obviously the polymer coil R_g governs the characteristic decay length in these cases. Addition of surfactant leads to changes in the hydrophobic−hydrophilic balance of the polymer coil, which would cause conformational changes in the polymer coil. In the case of SDS, for very small concentrations of surfactants, we have seen that the first interaction distance changes drastically. This obviously means that the added surfactant tends to associate with the polymer chains, which eventually leads to "stretched tail-like" conformation due to bound surfactant molecules. A schematic illustration of the intermediate stages of polymer−surfactant complexes is shown in Figure 8b. Here the individual surfactant molecules are shown by the small filled circle. The big thick circle represents the ferrofluid droplet which is about 200 nm in diameter. The hydrophobic tail of the surfactant molecule is not shown in the sketch. As the concentration increases, more and more surfactant molecules and micelles (above the critical aggregation concentration (cac) goes into the folded chains (loops) which stretch the loops further (Figure 8c). Earlier investigations[14,18] on the associative behavior of SDS on poly(ethylene oxide) is that the polymer adsorbed on the surface of SDS micelles. These micelles are slightly smaller than free micelles and are uniformly spaced on each polymer coil. The equilibrium spacing between the micelles on the polymer coil is governed by the balance of adsorption energy of the polymer segments and the electrostatic repulsion between the micelles. It has been found that within the aggregates there is strong repulsion between the polymer monomers, but as a whole it retains the unperturbed R_g of the polymer without micelles. What we have observed on the decay length from the force profile is consistent with small-angle neutron scattering experimental results (i.e., the R_g remains more or less the same). This observation also supports the earlier findings that at higher surfactant concentrations, the neutral polymer chains at the interface can be converted into partial polyelectrolyte complexes as a consequence of surfactant and polymer association.[23] In the case of polyelectrolytes,

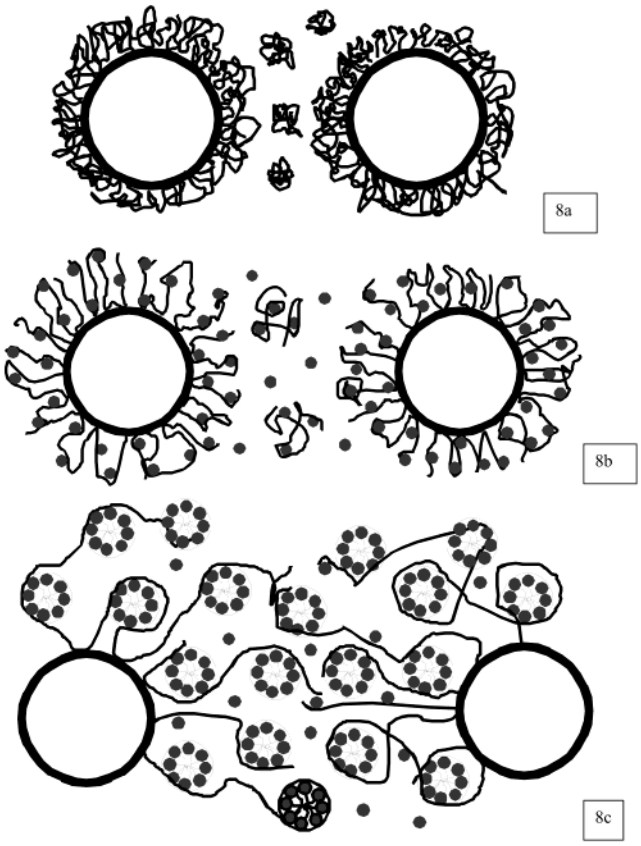

Figure 8. Schematic illustration of the polymer surfactant complexes: (a) Without any surfactant, the conformation of polymer at the droplet interface. Here, the adsorbed polymer adopts some arbitrary conformation with loops, trains, and tails. (b) Conformation of polymer−surfactant molecules, well below the cmc value, where the added surfactant tends to associate with the polymer chains leading to a "stretched tail-like" conformation. No micelles are present at this stage. (c) Conformation of polymer−surfactant complexes above the so-called cac. Under this condition, the neutral polymer chain at the interface behaves like a partial polyelectrolyte complex where the charges on the chain repel each other and the electrostatic repulsion collectively leads to chain stretching on length scales larger than the electrostatic blob size.

the charges on the chain, which repel each other, and the electrostatic repulsion collectively lead to chain stretching on length scales larger than the electrostatic blob size.[48,49] Probably this would explain the large shift in the onset of repulsion observed in our experiments, in the presence of polymer−surfactant complex, shown in Figure 6.

In the case of SDS, association begins at very low concentrations, whereas in the case of cationic surfactants, the association begins when the surfactant concentration is close to the cmc values. Therefore, it is clear that the association in the case of SDS is mainly because of the interaction between the polymer coils and the unimers of surfactant molecules. This was the main difference between anionic and cationic surfactants. Therefore, our experimental force profiles show that the surfactant−polymer binding process takes place above a certain concentration, depending on the nature of surfactant molecules and the droplet interface. Surfactant binding leads to strong modifications on the force profiles. Even at lower concentrations, the surfactant molecules bound

(48) de Gennes, P. G.; Pincus, P.; Velasco, R. M.; Forchard *J. Phys.* (*Paris*) **1976**, *37*, 1461.
(49) Rubinstein, M.; Colby, R. H.; Dobrynin A. *Phys. Rev. Lett.* **1994**, *73*, 2776.

to the polymer chains, as unimers, lead to changes in the conformation of adsorbed polymer. The stretched polyelectrolyte-like conformation of polymers due to its association with surfactant molecules and micelles can impart better stabilization (repulsion).

Conclusions

We have studied the forces between emulsion droplets in the presence of a neutral polymer and ionic and nonionic surfactants. The force profiles in the presence of an associative polymer follow an exponential scaling with a characteristic decay length, comparable to the R_g of the polymer. This decay length was weakly dependent on the surfactant concentration. The onset of the repulsive force dramatically increases with increase in surfactant concentration, suggesting that the adsorbed polymer coils adopt a stretched polyelectrolyte-like conformation due to association of surfactant molecules. These results suggest that the associative polymers can be potential candidates for making the emulsions stable for a sufficiently long period.

Acknowledgment. Authors wish to thank Shri. S. B. Bhoje, Director, Indira Gandhi Centre for Atomic Research, for his interest and support for this research program and Dr. S. L. Mannan, Associate Director, MDG, for encouragement. Support from Indo-French center for promotion of advanced scientific research (IFCPAR), New Delhi, is greatly acknowledged. J.P. is grateful to F. Leal-Calderon and J. Bibette for initiating this collaborative research program.

LA0256477